*Molecules* **2001**, *6*, 287–299

*molecules*
**ISSN 1420-3049**
http://www.mdpi.org

# Photooxidation of *n*-Hexanal in Air

**Jovan Tadić[1], Ivan Juranić[2] and Geert K. Moortgat[3]**

[1]Center for Chemistry IChTM, POB 815, Studentski trg 12-16, 11001 Belgrade, Yugoslavia, Tel. ++381-11-3236-603, Fax. ++381-11-639-827
[2] Faculty of Chemistry, University of Belgrade, POB 158, 11001 Belgrade, Yugoslavia
[3] Max-Planck-Institut für Chemie, Atmospheric Chemistry Department, Postfach 3060, 55020 Mainz, Germany
* Author to whom correspondence should be addressed; e-mail jtadic@Eunet.yu

*Received: 21 November 2000; in revised form 11 December 2000 / Accepted: 12 December 2000 / Published: 31 March 2001*

**Abstract**: Dilute mixtures of hexanal in synthetic air (up to 100 ppm) were photolyzed with fluorescent UV lamps (275-380 nm) in air at 298 K. The main photooxidation products, identified and quantitatively analyzed by FTIR spectroscopy, were butene, CO, vinylalcohol and ethanal. The photolysis rates and the absolute quantum yield Φ were found to be slightly dependent on the total pressure. At 100 Torr, $\Phi_{100}$ = 0.43 ± 0.02, whereas at 700 Torr the total quantum yield was $\Phi_{700}$ = 0.38 ± 0.02. These results may be explained by the collisional deactivations of photoexcited molecules. Two decomposition channels were identified: the radical channel $C_5H_{11}CHO \rightarrow C_5H_{11} + HCO$, and the molecular channel $C_5H_{11}CHO \rightarrow C_4H_8 + CH_2{=}CHOH$, having the relative yields of 27 and 73 % at 700 Torr. The product $CH_2{=}CHOH$ tautomerizes to ethanal.

**Keywords**: Photolysis, photooxidation, aldehydes.

## Introduction

Aldehydes play a significant role in a variety of atmospheric reactions, such as formation of photochemical smog, peroxyacetyl nitrate (PAN), and regional (tropospheric) ozone. Photodissociation of aldehydes represents an important source of free radicals in the lower atmosphere, and thus may significantly influence the atmospheric oxidation capacity [1-3]. Aldehydes are widely used in industry

and are the products of an incomplete combustion of petroleum fuels. Smaller alkyl aldehydes are also products of the atmospheric photooxidation of hydrocarbons, ethers, alcohols, and other organic compounds. Vegetation, biomass and other living organisms emit many of these compounds: *n*-hexanal and higher aldehydes have been observed in ambient air and in emissions of various plants, especially grasses, with comparable emissions rates as the monoterpenes [4,5].

Aldehydes absorb in the near UV range, and dissociate upon absorption of light. Aliphatic aldehydes exhibit a weak absorption band in the wavelength range 240-360 nm as a result of a symmetry forbidden $n$ - $\pi^*$ transition [6,7]. Photodissociation of aldehydes produces free radicals, which are subsequently involved in other atmospheric reactions and reaction cycles. There have been a number of studies devoted to the photodissociation of the simplest alkyl aldehydes, such as HCHO, $CH_3CHO$, $C_2H_5CHO$ [8-16], but a relatively small number devoted to longer chain aldehydes, such as $C_3H_7CHO$, $C_4H_9CHO$ [17,18] and *iso*-pentanal and *tert*-pentanal [32].

Photolysis of *n*-hexanal could theoretically occur according to the several suggested reaction schemes for *n*-pentanal [18], where processes (1) and (3) are thought to be the most important:

| | | | | |
|---|---|---|---|---|
| $CH_3CH_2CH_2CH_2CH_2CHO + h\nu$ | $\rightarrow$ | $n\text{-}C_5H_{11} + HCO$ | (Norrish Type I) | (1) |
| | $\rightarrow$ | $n\text{-}C_5H_{12} + CO$ | | (2) |
| | $\rightarrow$ | $C_4H_8 + [CH_2{=}CHOH]$ | (Norrish Type II) | (3) |
| | $\rightarrow$ | $C_3H_7 + CH_2CH_2CHO$ | | (4) |
| | $\rightarrow$ | $C_5H_{10} + HCHO$ | | (5) |
| | $\rightarrow$ | $CH_3CH_2CH_2CH_2CH_2CO + H$ | | (6) |

Process (1) represents the fragmentation into free radicals, with an enthalpy of around 350 kJ/mol corresponding to a photochemical threshold of around 340 nm [18]. Process (3), which is common to molecules with a γ-hydrogen atom, is an intramolecular rearrangement with enthalpy around 80 kJ/mol ($\lambda \leq 1454$ nm) [18]. The enthalpy for process (3) was calculated assuming that the keto-form of acetaldehyde is formed in the primary step. As a matter of fact, this assumption is not correct, and, therefore, enthalpy for these reactions should be changed for the difference between the heats of formation of enol and keto forms of acetaldehyde (the pK value for keto-enol equilibrium is ~7 and the corresponding $\Delta G$ value is ~18 kJ/mol) [33].

There is also a theoretical possibility for the *n*-hexanal molecule to undergo photocyclisation, forming *cis/trans* isomers of 2-ethyl-cyclobutanol (Scheme 1). These compounds were not detected in our experiments.

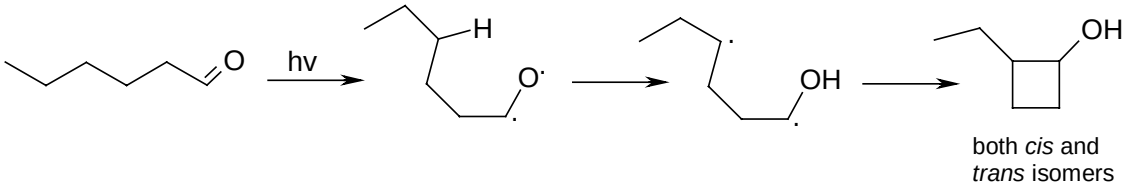


**Scheme 1.**

In this paper, the results obtained from the photolysis of small quantities of *n*-hexanal in air, using wide band emission lamps, are reported. We have investigated products and absolute quantum yields in the pressure range 100 to 700 Torr.

The photooxidation experiments were carried out in a long-path quartz cell with detection of precursors and products by FTIR spectroscopy. After identification and quantification of the products, a mechanistic description of the photooxidation/photolysis was deduced. From the measured decay rate of the starting material, and from the knowledge of the absorption spectrum, overall quantum yields for the photolysis were calculated for various pressures.

## Results and Discussion

### *Photolysis of n-Hexanal*

Figure 1 shows the FTIR spectra of a mixture of 100 ppm *n*-hexanal in synthetic air, before and after the photolysis, and the differential spectrum. Major products were found to be CO ($\nu_{max}$ = 2037-2235 $cm^{-1}$), 1-butene (911.5 $cm^{-1}$), ethenol (vinyl alcohol) being the enol form of ethanal (947.6 $cm^{-1}$, 1078 $cm^{-1}$, 1118.3 $cm^{-1}$, 1259.8 $cm^{-1}$), ethanal (1348.5-1355.5 $cm^{-1}$) and $CO_2$ (2290-2384 $cm^{-1}$). The latter compound is considered as an artifact, and is unavoidably produced from desorption from the wall.

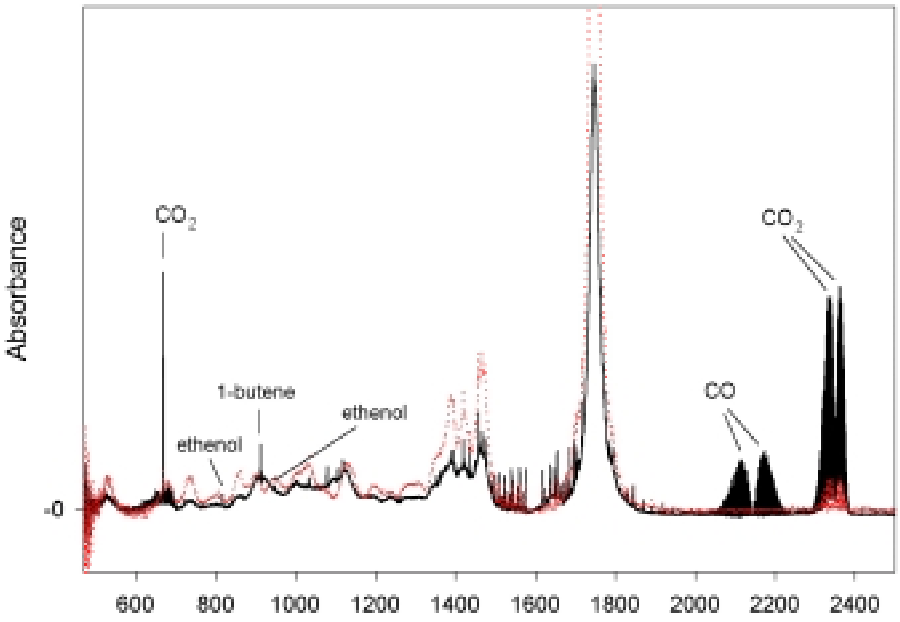


**Figure 1.** IR spectrum of 100 mTorr *n*-hexanal, before and after photolysis (6 TL/12 lamps, 100 Torr synthetic air). The differential spectrum is also shown below. Major products CO, 1-butene, and ethanol, and $CO_2$ as a by-product, are marked (exact positions of the peaks are given in the main text).

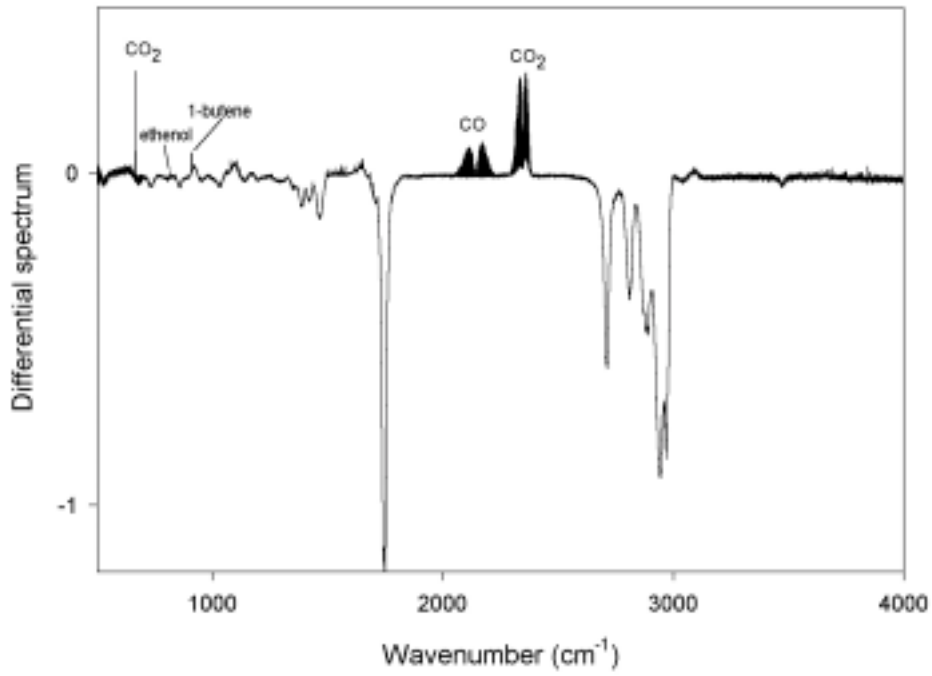


Figure 2 shows the concentration-time profiles for the various products.

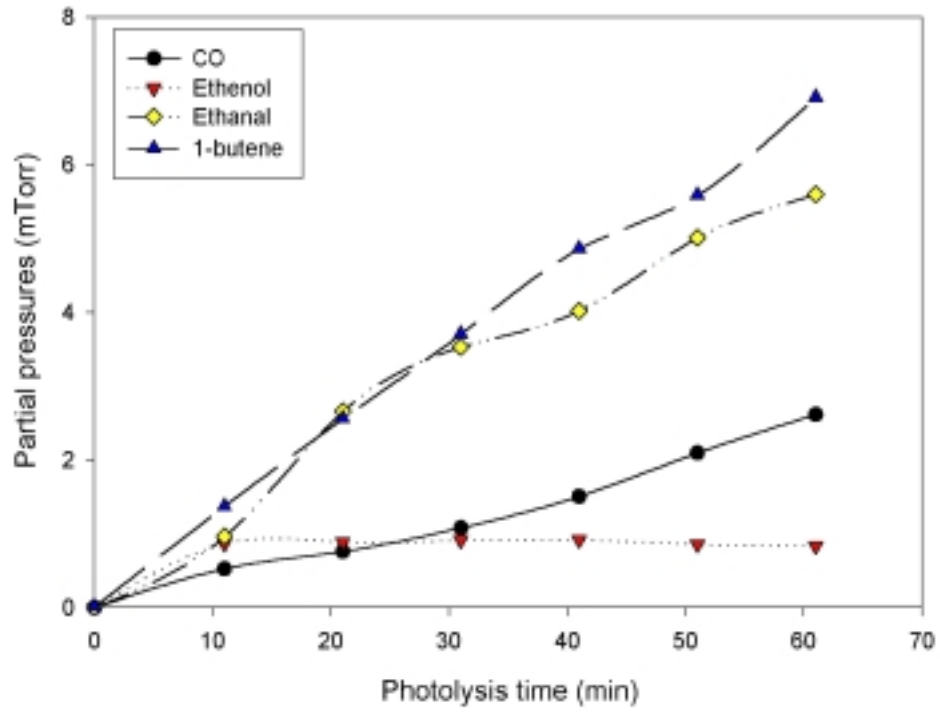


**Figure 2.** Photolysis of *n*-hexanal: time profile - variation of the concentrations of products. The CO curve shows that it is not only the primary product, but also a product of the reactions following primary step. Ethenol partial pressure reaches maximum and then starts to decrease by conversion to ethanal, which is in good agreement with simulation of the process.

From the observed products, it seems evident that only Norrish Type I and II processes occur, and the proposed mechanism would be:

$$CH_3CH_2CH_2CH_2CH_2CHO \rightarrow CH_3CH_2CH_2CH_2CH_2 + HCO \quad (1)$$
$$\rightarrow CH_2{=}CHCH_2CH_3 + CH_2{=}CHOH \quad (3)$$

1-Butene is purely primary product that can be expected in this reaction system. Ethanal is secondary product arising from ethenol conversion, and undergoes further photolysis.

Reaction (2), also producing CO, does not take place, since a co-product of the reaction, *n*-$C_5H_{12,}$ was not detected during the photolysis. Reaction (1) gives two radicals, which immediately react with oxygen. The formyl radical HCO is quantitatively converted to CO and $HO_2$ [26-28], according to

$$HCO + O_2 \rightarrow HO_2 + CO$$

allowing the usage of the primary produced CO as the indicator for process (1). *n*-Pentyl radicals also subsequently react with oxygen, forming *n*-pentylperoxy radicals,

$$n\text{-}C_5H_{11} + O_2 \rightarrow n\text{-}C_5H_{11}O_2$$

The fate of the *n*-$C_5H_{11}O_2$ radicals is to react with $HO_2$, or to disproportionate, to produce a variety of products [29,30]

$$2\ n\text{-}C_5H_{11}O_2 \rightarrow 2\ n\text{-}C_5H_{11}O + O_2$$
$$\rightarrow n\text{-}C_5H_{11}OH + n\text{-}C_4H_9CHO + O_2$$
$$n\text{-}C_5H_{11}O + O_2 \rightarrow n\text{-}C_4H_9CHO + HO_2$$
$$n\text{-}C_5H_{11}O_2 + HO_2 \rightarrow n\text{-}C_5H_{11}OOH + O_2$$

However due to the estimated low reaction rate constant for the disproportionation [30], the major expected product would be *n*-pentyl-hydroperoxide (*n*-$C_5H_{11}OOH$). The latter compound (also *n*-pentanal, and *n*-pentanol) was below the detection limit of the applied analytical method (less than 1 mTorr). Also no evidence was found for the presence of products of other possible channels.

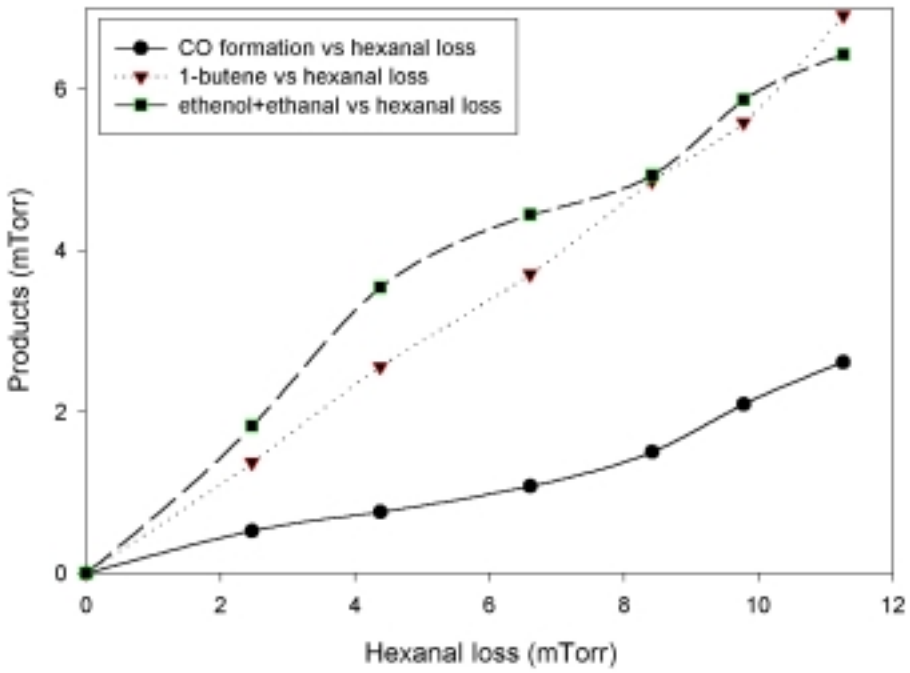


**Figure 3.** Photolysis of *n*-hexanal - products formation versus loss in *n*-hexanal. See comments on Figure 2.

1-Butene is a stable molecular species and was used as the indicator for the process (3). The co-product of reaction (3) is the formation of the ethenol $CH_2$=CHOH, which tautomerizes slowly to ethanal. This is clearly seen in Figure 2, where the concentration-time profile of the enol product displays the behavior of a primary product. Ethenol concentration reaches a maximum after 10 minutes photolysis, and its subsequent decay is connected with its conversion to ethanal. Figure 3 shows profiles of products concentrations (partial pressures) of CO, 1-butene and the sum of ethenol and ethanal *versus* loss of *n*-hexanal. According to the suggested mechanism, the yield of 1-butene is (within experimental error) nearly identical with the sum of yields of ethenol and ethanal, since both compounds are products of the same decomposition channel. CO is mainly a primary product, but small increases of the yield at long conversion times is observed, which can be attributed to the photolysis of secondary products such as ethanal.

The relative probability for *n*-hexanal molecule to undergo two detected decomposition channels is shown in the Table 1. The probability is deduced from the ratio of primary formed CO (Norrish Type I), and 1-butene (Norrish Type II). This method is chosen to overcome the inability of measuring absolute initial concentrations of the sticky substance, because of the loss of the substance on the walls of gas-handling system before the substance is introduced to the reactor. This means that uncertainty is

presented in determining initiall concentration of the *n*-hexanal after it is introduced in the main cell (the rate is still clear, because there is no wall loss after introduction).

**Table 1.** Probabilities for *n*-hexanal molecule to undergo different decomposition channels, TL12 lamps (errors are represented by experimental scatter).

| Total pressure (Torr) | Norrish type I | Norrish type II |
|---|---|---|
| 100.00 | 0.35 | 0.66 |
| 100.00 | 0.38 | 0.62 |
| 100.00 | 0.35 | 0.65 |
| | 0.36±0.02 | 0.64±0.02 |
| 300.00 | 0.28 | 0.72 |
| 300.00 | 0.26 | 0.74 |
| 300.00 | 0.28 | 0.72 |
| | 0.27±0.01 | 0.73±0.01 |
| 500.00 | 0.29 | 0.71 |
| 500.00 | 0.29 | 0.71 |
| 500.00 | 0.30 | 0.70 |
| | 0.29±0.01 | 0.71±0.01 |
| 700.00 | 0.27 | 0.73 |
| 700.00 | 0.28 | 0.72 |
| 700.00 | 0.27 | 0.73 |
| | 0.27±0.01 | 0.73±0.01 |

The relative yields for the different products observed are summarized in Table 2. Assuming that the formation of $CO_2$ is an artifact, the sum of both processes Norrish Type I and II is approximately 0.82 ± 0.05, which would indicate that additional products might be formed by other processes.

**Table 2.** Relative yields of different products in typical *n*-hexanal photolysis experiment, TL/12 lamps (done by quantifying *n*-hexanal using UV measurement of it)

| Δ CO/ -Δ hexanal | Δ 1-butene / -Δhexanal | Δ **(**ethanal+ethenol )/ -Δhexanal |
|---|---|---|
| 0.23 | 0.61 | 0.57 |

Speculation about the formation of 2-ethyl-cyclobutanol is based on the mechanism of the formation of an analogous product, 2-methyl-cyclobutanol, formed in the photooxidation of *n*-pentanal [25], although we have found no evidence for it.

*Absolute Quantum Yields*

One of the objectives of the study was to determine the absolute quantum yield dependency on the total pressure. Chlorine was used as the actinometer. From the decay of *n*-hexanal concentration, the photolytic rate constants were deduced for the different pressures by plotting the natural logarithm of concentration versus time (first order decay), and performing a least-square fit. From these results, overall quantum yields were calculated according to the Equation (1) using the overlap integrals of *n*-hexanal and chlorine spectra within the range of the TL/12 emission (280-360 nm, see Fig. 5). In all cases the absolute quantum yield dependency on the total pressure was observed. The data are summarized in Table 3 for experiments performed at a total pressure of 100, 300, 500 and 700 Torr and also shown in form of a Stern-Volmer presentation in Figure 4. Since the intercept at zero pressure is not equal to 1 (the intercept is 2.26), as should be expected if collisional deactivation is the only relaxation process beside the photodecomposition, it seems very probably that there are other energy-dissipating processes (the triplet state of *n*-hexanal could deactivate by phosphorescence etc.). The interaction with the walls moving to the ground state is of minor importance becase of huge volume to surface ratio. The slope of the fit, described by $4.758 \times 10^{-4}$ x P corresponds to the sensitivity of absolute quantum yield on the total pressure P.

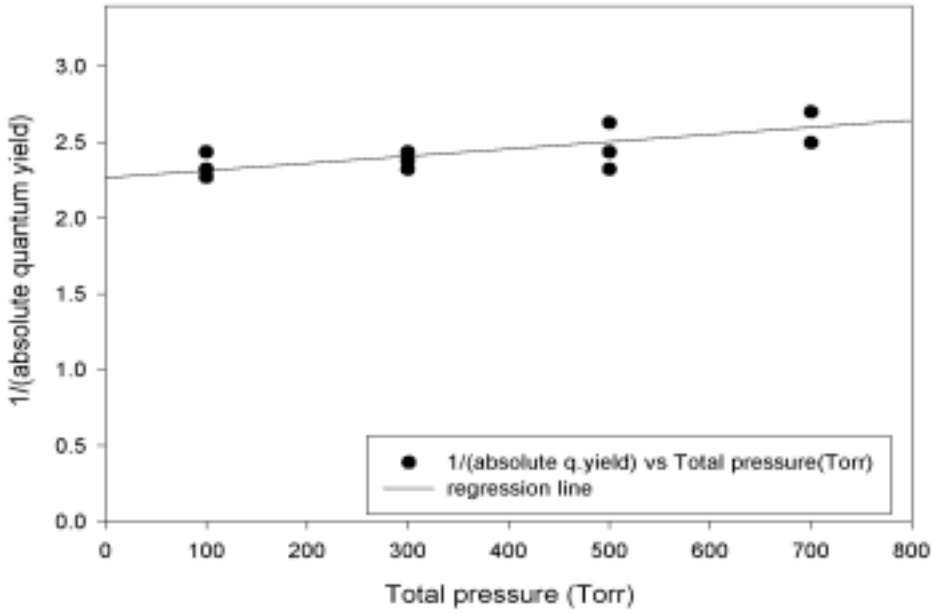


**Figure 4.** The pressure dependency of 1/(absolute quantum yields) in *n*-hexanal photolysis, at different total pressures of synthetic air (Stern-Volmers plot). If collisional deactivation is the only relaxation process, one should expect that the interception on the ordinate should be one. This is not the case, indicating that one or more other energy dissipating processes from photoexcited molecules are taking place. Possible explanations are given in the main text.

The total quantum yield Φ can be calculated from the following equation $1/\Phi = 2.26 + (4.758 \times 10^{-4})P$**.** Using the estimated relative quantum yield from Tables 1 and 2, it is possible to estimate the absolute contribution at atmospheric conditions (700 Torr): for Norrish type I (radical) process, φ(I) = 0.08 and Norrish Type II (molecular) φ(I) = 0.23 (total quantum yield being 0.38, and a contribution of both decomposition channels being 82 %).

**Table 3.** Absolute quantum yield values *n*-hexanal photolysis at different pressures of synthetic air (errors are represented by experimental scatter).

| Pressure (Torr) | Abs. Quantum yield |
|---|---|
| 100.00 | 0.43 |
| 100.00 | 0.41 |
| 100.00 | 0.44 |
| | **0.43 ± 0.02** |
| 300.00 | 0.41 |
| 300.00 | 0.42 |
| 300.00 | 0.43 |
| | **0.42 ± 0.01** |
| 500.00 | 0.43 |
| 500.00 | 0.38 |
| 500.00 | 0.41 |
| | **0.40 ± 0.03** |
| 700.00 | 0.40 |
| 700.00 | 0.37 |
| 700.00 | 0.37 |
| | **0.38 ± 0.02** |

## Conclusions

In this work we achieved several goals:

· Identification of the products of hexanal photolysis, detectable in IR region under applied conditions.
· Quantification of the products, and deduction of the photodecomposition pattern, particularly of primary step, exploiting the benefit of applied experimental system
· Determination of the absolute quantum yields at different pressures, providing values necessary for atmospheric modeling, at the same time examining the influence of the total pressure on the absolute quantum yield, evaluating importance of collisional deactivations, and indicating other relaxation channels

There is evidence that up to C4 aldehydes the decomposition upon absorption of light mainly follows the free radical channel (Norrish type I), forming formyl radical and alkyl radical [25,31]. The higher than C4 aldehydes, starting with pentanal, mainly decompose by internal rearrangement of the molecule (Norrish type II), forming vinyl alcohol, and the corresponding 1-alkene. Our results strongly support this pattern. There is no conclusive evidence for the formation of cyclobutanol derivatives, and further examinations on the subject should be done.

## Experimental

The apparatus employed in this work has been described elsewhere [19-20] and will be briefly discussed here. The central part of the apparatus is a 44.2 liter (1.40 m length and 20 cm diameter) quartz cell equipped with two independent sets of White-optic mirror arrangements. Sapphire-coated aluminum mirrors were used in the infrared region ($l$ = 33.6 m) for the measurements of the educts and products. A set of $MgF_2$-coated mirrors was used in the UV/visible region ($l$ = 9.82 m), for measuring the photolysis rates of the actinometer, $Cl_2$. Infrared spectra at 0.5 $cm^{-1}$ resolution (450-4000 $cm^{-1}$) were measured with a Bomem DA8-FTIR spectrometer. For the UV measurements the same diode array detector as previously described [20-22] was used. This method provides the possibility of simultaneous detection and monitoring of all the IR-active products and the starting material.
Photolysis was achieved with six radially mounted lamps, TL/12-sunlamps (Philips 40W TL/12 lamps (275-380 nm).

Spectra were taken every 5 -10 min. with total irradiation time of 30-50 min. Extent of the conversion of initial compound was approximately 30 %.

The use of a continuous broad band light source allows only the determination of an integral, effective quantum yield $\Phi^{int}$ for the photoactive spectral region. Quantum yields were calculated according to the following equation[20] (for carbonyl compound, C, and actinometer, Act):

$$\Phi^{int}(C) = \frac{K_{phot}(C)}{K_{phot}(Act)\dfrac{\Sigma\, OV(C)}{\Sigma\, OV(Act)\cdot\Phi^{int}(Act)}}$$

**Equation 1.**

For all TL/12-experiments, chlorine was used as actinometer (with $\phi$ = 1), using ethane as Cl-atom scavenger**.** The quantum yield is the single unknown parameter in the equation. The photolysis rates for both compound $K_{phot}(C)$ and actinometer $K_{phot}t(Act)$ could be directly measured, and the terms $\Sigma$OV(C) and $\Sigma$OV(Act) represent the calculated overlap of lamp emission and absorption spectrum of substrate. Figure 5 displays the emission spectra of the lamps and the spectrum of $Cl_2$.

The knowledge of the UV absorption spectra of hexanal was a basic prerequisite for these experiments. The absorption spectrum has been recently measured [23], and is very similar to the homologous aldehydes, butyraldehyde and pentanal [24,25]. The spectrum displays a broad absorption band between 250 and 350 nm, with a maximum at 295 nm with cross section of 6.0 x $10^{-20}$ $cm^2$ $molecule^{-1}$. For comparison the spectra butanal and pentanal are also given in Figure 5.

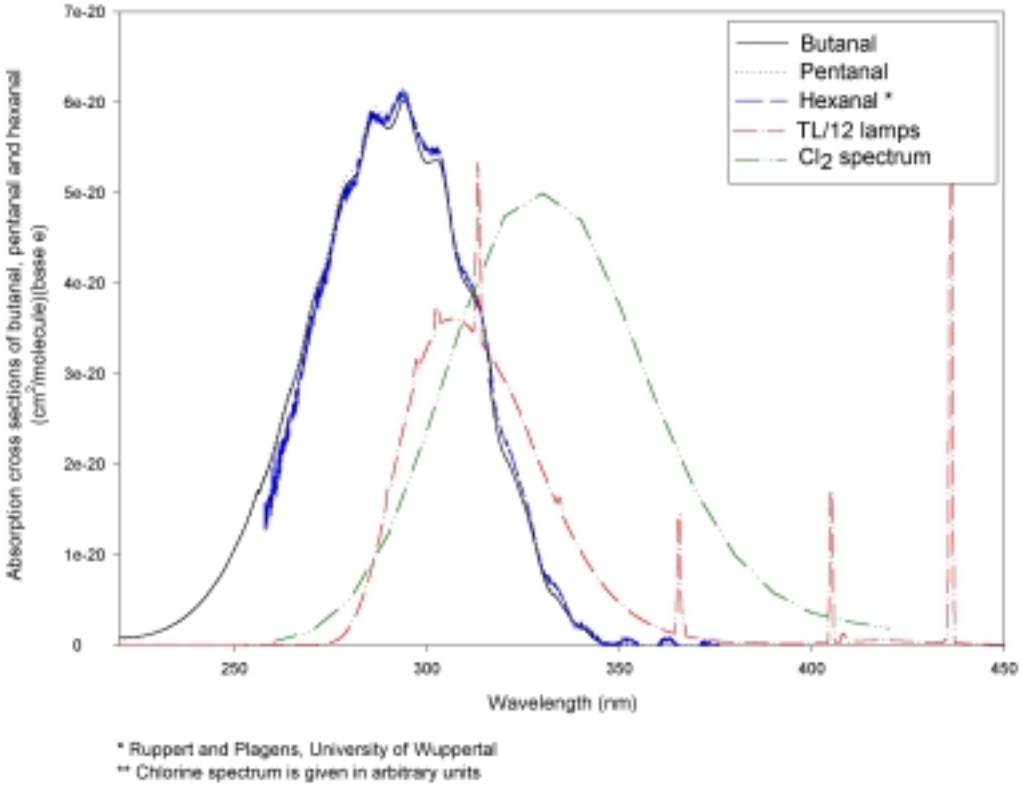


**Figure 5.** Emission spectrum of photolysis lamps (TL12/Philips), absorption spectrum of $Cl_2$ and cross section of *n*-hexanal [23]. Cross sections of butanal and pentanal are also given for comparison. Figure explains why chlorine was used as actinometer, and why TL12 lamps were chosen for photolysis, since there is a good overlap of all three regions.

Experiments were carried out at room temperature (298 K), at pressures between 100 to 700 Torr (1 Torr = {101325/760}Pa), with an initial concentrations of approx. 100 ppm. Qualitative and quantitative data evaluation was carried out by comparing the products spectra with reference spectra obtained in the same cell and using calibration curves at corresponding pressures and resolution.

Carbonyl compounds were obtained from Sigma-Aldrich Company with purity higher than 98%. Before use, all samples were degassed by several freeze-pump-thaw cycles. Purity of the compounds was checked by FTIR spectral measurements and no impurities were found. The calibration of vinyl

alcohol was done indirectly, from the amount of formed ethanal and the converted vinyl alcohol (peak decrease), since the conversion of these compounds is 1:1 (keto-enol tautomerism) according to:

$$CH_2=CH\text{-}OH \rightleftharpoons CH_3\text{-}CH=O$$

**References and Notes**


1. Graedel, T.E.; Farrow, L.A.; Weber, T.A. *Atmos. Environ.* **1976**, *10*, 1095-1099.
2. Grosjean, D. *Environ. Sci. Technol.* **1982**, *16*, 254-259.
3. Finlayson-Pitts, B.J.; Pitts, J.N., Jr. *Atmospheric Chemistry*; John Wiley: New York, **1986**.
4. Owen, S.; Boissard R.; Street R.A.; Duckam S.C.; Csiky, O.; Hewitt C.N. *Atmos. Environ.* **1997**, *31 S1*, 101-105.
5. Kirstine, W.; Galbally, I. *J. Geophys. Res.* **1998**, 103, 10603-10607.
6. Calvert, J.G.; Pitts, J.N., Jr. *Photochemistry*; John Wiley: New York, **1966**; pp 372-375.
7. Lee, E.K.C.; Lewis, R.S. *Adv. Photochem.* **1980**, *12*, 1-7.
8. Moortgat, G K.; Seiler, W.; Warneck, P. *J. Chem. Phys*. **1983**, *78*, 1185-1191.
9. Carmely, Y.; Horowitz, A. *Int. J. Chem. Kin.* **1984**, *16*, 1585-1589.
10. Moore, C.B.; Weishaar, J.C. *Annu. Rev. Phys. Chem.* **1983**, *34*, 525-532.
11. Ho, P.; Bamford, D.J.; Buss, R.J.; Lee, Y.T.; Moore, C.B. *J. Chem. Phys.* **1982**, *76*, 3630-3635.
12. Horowitz, A.; Calvert, J.G. *J. Phys. Chem.* **1982**, *86*, 3105-3111.
13. Meyrahn, H.; Moortgat, G.K.; Warneck, P.; Presented at the *15th Informal Conference on Photochemistry*, Stanford, CA, July, **1982**.
14. Shepson, P.B.; Heicklen, J. *J. Photochem.* **1982**, *19*, 215-220.
15. Heicklen, J.; Desai, J.; Bahta, A.; Harper, C.; Simonaitis, R. *J. Photochem.* **1986**, *34*, 117-121.
16. Terentis, A.C.; Knepp, P.T.; Kable, S.H. *J. Phys. Chem.* **1995**, *99*, 12704-12709.
17. Forgeter, S., Berces, T., Dobe S. *Int. J. Chem. Kin.* **1979**, *11*, 219-237.
18. Cronin, J.T.; Zhu, L. *J. Phys. Chem. A* **1998**, *102*, 10274-10279.
19. Moortgat, G.K.; Cox, R.A.; Schuster, G.; Burrows, J.P.; Tyndall, G.S. *J. Chem. Soc. Farad. Trans. II* **1989**, *85*, 809-818.
20. Raber, W.H.; Moortgat, G.K. *Adv. Ser. in Phys. Chem., 3, "Progress and Problems in Atmospheric Chemistry"*, Ed. J.R. Barker, Word Scientific Publ. Co., Singapore, **1995**, 318-373.
21. Crowley, J.N.; Moortgat G.K. *J. Chem. Soc. Farad. Trans.* **1992**, *88*, 2437-2448.
22. Meller, R.; Raber, W.; Crowley, J.N.; Jenkin, M.; Moortgat, G.T. *J. Photochem.* **1991**, *A62*, 163-174.
23. Plagens, H.; Bröske, R.; Splitter M.; Ruppert L.; Barnes I.; Becker, K.H. *Proceedings of the Second Workshop of the Eurotrac-2 Subproject CMD, "Chemical Mechanism Development"*, 23-25-September **1998**, Karlsruhe.
24. Martinez, R.D.; Buitrago, A.A.; Howell, N.W.; Hearn, C.H.; Joens, J. A. *Atmos. Environ.* **1992**, *26*, 785-794.

25. Moortgat, G.K., Final report on EU project RADICAL: ”Evaluation of radical sources in atmospheric chemistry through chamber and laboratory studies” ENV4-CT97-0419, March **2000**.
26. Moortgat, G.K.; Seiler, W.; Warneck, P. *J. Chem. Phys.* **1983**, *78*, 1185-1193.
27. Horowitz, A.; Calvert, J.G. *Int. J. Chem. Kin.* **1978**, *10*, 805-813.
28. Horowitz, A.; Su, F.; Calvert, J.G. *Int. J. Chem. Kin.* **1978**, *10*, 1099-1108.
29. Atkinson, R. *J. Phys. Chem. Ref. Data*, **1994**, Monograph 2,
30. Lightfoot, P.D.; Cox, R.A.; Crowley, J.N.; Destriau, M.; Hayman, G.D; Jenkin, M.E.; Moortgat, G.K.; Zabel, F. *Atmos. Environ.* **1992**, *26A*, 1805-1811.
31. Tadic, J.; Moortgat, G.K. Manuscript in preparation.
32. Zhu, L.; Cronin, J.T.; Narang A. *J. Phys.Chem.A* **1999**, *103*: 36, 7248 - 7253.
33. Bell R.P.; Smith P.W. *J. Chem. Soc. (B)* **1966**, 241-248.

*Sample Availability*: Not available